University of Nevada, Reno

Monitoring the Optical Decay of a Black Hole

X-ray Binary using the Great Basin Observatory

A senior thesis submitted in partial fulfillment of the requirements for the degree of Bachelor of

Science in Physics

By

Sarah L. Colangelo

Dr. Richard Plotkin/Senior Thesis Advisor

Dr. Melodi Rodrigue/Reader

May, 2020

1 Abstract

Low mass X-ray binary (LMXB) systems are composed of a stellar black hole and a companion star that powers the black hole by accretion. These types of systems spend a majority of the time in a state of quiescence, but have been observed to enter an outburst cycle. The LMXB binary system MAXI J1820+070 was observed as it was going through an outburst cycle beginning in the hard state and transitioning into the soft state before entering quiescence again. Observations in the optical light spectrum began towards the end of the outburst cycle in October of 2018 with the use of the Great Basin Observatory. The brightness of the system was monitored regularly to determine how the optical light emitted during the outburst changes over time which resulted in a decay timescale of 43 days. This result was compared to that of the X-ray light emitted from the same source in order to better understand the complex structure of the black hole system.

2 Introduction- Background

Binary systems are systems in which two or more objects interact and orbit around a common center of mass. The primary object, typically the more massive object in the system, is most commonly a star but has also observed to be a white dwarf, neutron star, or black hole.

The nature of the primary object influences how the objects in the binary system will interact with one another [6]. Three types of interacting binaries are detached, semi-detached, and contact and are all characterized based on how the objects evolve with respect to one another over time. In each of the interacting systems, the shape of the objects experiences distortion due to the effects of gravitational and tidal forces between the objects. This distortion is related to the relative distances of the objects and their respective radii. A mass element of an object with mass

M_1 will feel a gravitational force on the surface at a distance Δr from the center due to the object itself as well as a tidal force due to a second object of mass M_2 at a separation distance of r [6]. The effect of these forces causes the shape of the masses to distort and form a more oval shape rather than circular shape, and as the ratio of $\Delta r/r$ increases, the effect of the tidal forces increases. The surrounding region of space of these objects forms a "figure 8" meaning the regions join at a pinched point called the Roche lobe. This description is shown in Figure 1.
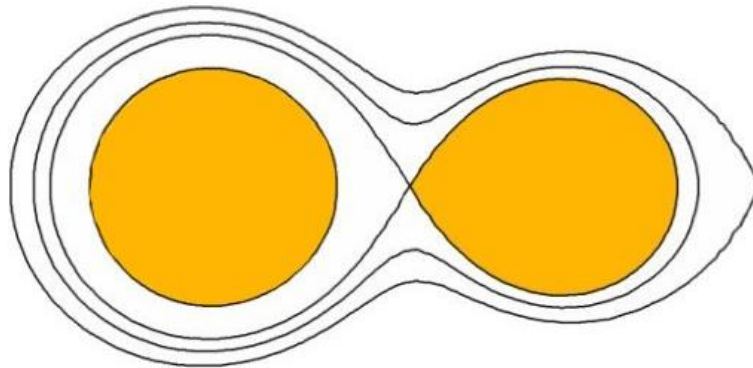
In a semidetached system, one star fills its Roche lobe while the other is smaller than the Roche lobe.

Figure 1: This figure [5] shows how an object fills the Roche lobe in a semi-detached binary to transfer matter via accretion. The stars are located at the center of the orange regions.

How an object fills the Roche lobe with material determines what type of interacting binary system it is. If neither object fills its Roche lobe, the system is defined as a detached binary, whereas if only one of the objects fills its Roche lobe, it is defined as a semi-detached binary [6]. A contact binary system occurs when both objects fill their Roche lobes with material. Material from a semi-detached binary will always transfer from the filled Roche lobe to the companion object powering it by accretion as illustrated in Figure 1. Accretion is the process

in which matter falls onto another object typically resulting in the release of large amounts of radiation as gravitational potential energy of the matter is lost during its freefall.

Black holes are objects with significant mass and infinitesimal radii causing extreme gravitational forces. Within the event horizon of a black hole, the gravity is so great that the escape velocity is greater than the speed of light which means nothing, including photons, can escape the gravitational pull of a black hole. In the event of a black hole binary system, the black hole is powered by accretion in that all the material that accumulates in a disk (accretion disk) around the object will eventually lose enough energy and angular momentum that it falls into the black hole. This allows radiation to be generated without nuclear reactions [6]. Black hole binary systems vary depending on the size of the black hole. There are stellar, intermediate, and supermassive black holes, all of which are categorized based on their masses. Stellar black holes have masses in the range of around 3 to 10 solar masses while supermassive black holes have masses that are millions or even billions of solar masses. Intermediate black holes exist in the range between stellar and supermassive black holes.

Low-mass X-ray binary (LMXB) systems are highly energetic and contain a black hole that is on the order of one solar mass along with a low mass companion star [4]. LMXB spend most of the time in a state of quiescence meaning little to no X-rays are detected. Some LMXB systems known as transient or outbursting systems experience sudden changes to their brightness and are detected as the outburst transitions between hard and soft states. The hard and soft states correspond to changes in the accretion flow which is modeled by a hardness-intensity diagram (HID) [3]. Figure 2 displays an example of a HID and the "q" shape the outburst follows.
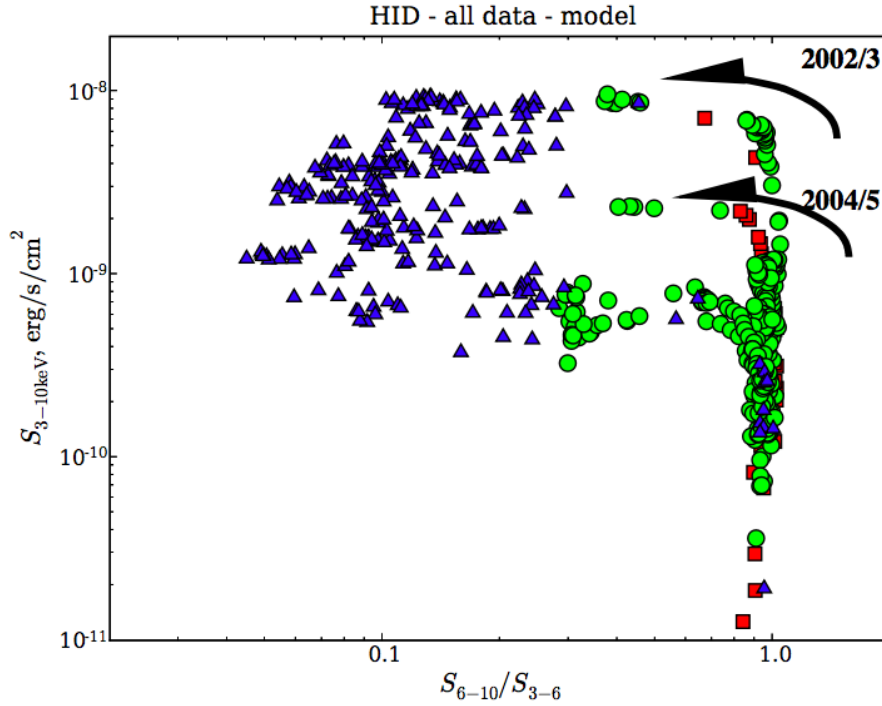
Figure 2: The HID [3] displayed is a composition of two different outbursts from the black hole binary GX 339-4 and demonstrates the general pattern observed by a transient X-ray outburst. The x-axis represents the hard to soft ratio and the y-axis represents the X-ray flux. The green points indicate the transition between hard to soft X-rays and the blue indicate the transition between soft to hard.

As the LMXB goes through outburst cycles, the temperature of the accretion flow varies across the corona and accretion disk. The temperature of the disk decreases as the distance from the black hole increases. This is due to less emission of highly energetic X-rays and more emission of less energetic electromagnetic radiation such as ultraviolet and optical rays. Figure 3 models the structure of the corona and accretion disk illustrating where the majority of the electromagnetic radiation is located.
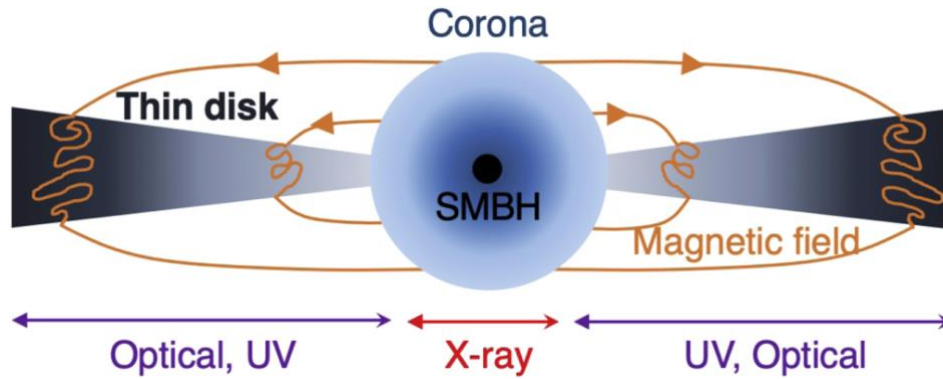
Figure 3: This illustration [8] shows the general structure of the accretion disk of a black hole and how the electromagnetic radiation varies along the disk. The more energetic X-rays reside closer to the corona of the black hole while the less energetic ultraviolet and optical radiation exist farther from the corona.

The goal of this thesis is to observe the optical emission of a LMXB during the end of an outburst cycle as it transitions back to quiescence and how the brightness, or magnitude, of the system changes over time. Using this information, a comparison of the optical region of the accretion disk can be made with respect to the ultraviolet and X-ray regions. A secondary goal from the data is to investigate how the optical light decays compared to the decay of the X-ray light through the outburst to give some insight as to how the complex structure of the corona and accretion disk evolve over time.

3 Introduction- Source

The source MAXI J1820+070 (J1820), also known as ASASSN-18ey, is a LMXB with a companion star that has a mass roughly that of one solar mass and experiences mass transfer through Roche lobe overflow [10]. This source was discovered as an optical transient on March 6, 2018 by the All-Sky Automated Survey for Supernovae as well as an X-ray transient by the

Monitor of All-sky X-ray Image (MAXI) [9]. Using the method of parallax, the distance to the source was precisely calculated at 2.96 ± 0.33 kpc, and by using this distance other characteristic quantities such as jet velocity and inclination, mass, and luminosity have been more refined. As a result of the determination of the distance, the mass of the black hole has been estimated to be approximately 9.5 ± 1.4 solar masses [1]. Another important characteristic quantity is that this system has a magnitude of 14.2.

The data collected from the J1820 source for this project was done by using the remote telescope at the Great Basin Observatory (GBO) located in the mountains of the Great Basin National Park in eastern Nevada. This secluded location offers ideal conditions to operate a telescope free from pollution of cities and large populations. The observatory uses a 0.7-meter diameter reflecting telescope attached with a SBIG STX-16803 CCD camera [7]. The telescope takes observations in the visible, or optical, light range and for this project images in the r' filter, a variation of the R filter at an effective wavelength of 6122 angstroms [2], were used.

Observations of J1820 were taken regularly, nearly every two nights, beginning October 13, 2018 until October 24, 2018. The corresponding Modified Julian Dates (MJD) are MJD 58415 and MJD 58426. The source was then revisited in late April of 2019 and early May of 2019. The dates of observations were chosen as the source was going through an outburst cycle beginning in the hard state and progressing into the soft state during this time. The source was revisited when it was observed to enter the hard state of the outburst once again. The data recorded by MAXI began on MJD 58300 until about MJD 58400, so the data collected by GBO occurred after the X-rays could no longer be detected by MAXI. The data used for this project was obtained from the end of the initial outburst in October 2018.

4 Observations/Data Analysis

The data that was collected from GBO included 105 raw, or science, images in the r'

filter along with a set of calibration images. The science images were taken over the course of a

week beginning on October 13, 2018 and ending October 24, 2018 with each night of

observations collecting 15 science images at two minute exposures. The dates of observations

were chosen as J1820 was observed to be transitioning into quiescence at the end of the initial

outburst.

The calibration images include a bias, a dark, and a flat frame that were used to calibrate

each of the science images. A bias frame is obtained by taking an image at zero second exposure

with the purpose being to subtract out extra counts that have been artificially added to each pixel

of the detector. Dark frames work to subtract out the inherent thermal noise in the detector and

are obtained by taking an image with a cover over the camera set to the same exposure time as

the science images taken. A flat frame is created by imaging a uniform light source to later

divide out the variations in the optical system and to normalize the pixels across the detector. A

script written in Python performed the image calibration according to equation 1:

$$\text{calibrated\_image} = (\text{science\_image} - \text{bias\_frame} - \text{dark\_frame}) / \text{flat\_frame} \qquad (1)$$

An important note is the bias frame was subtracted from the dark frame before applying this

equation to the science images, as the dark frames included the bias within them.

Further analysis was conducted by hand and upon manual inspection of the images, the

target was clearly detected in the individual two minute exposures. This means that the signal to

noise ratio is small enough that the information gathered from one image per night is sufficient.

The purpose of such a large dataset is to help reduce the signal to noise ratio, but because the ratio was small enough, only one image per night was analyzed, otherwise analysis of the full dataset would be unrealistic for this project.

To begin analyzing the calibrated images, an imaging software called SAOImageDS9 (DS9) was used. Using DS9, differential photometry was performed on the images to produce a light curve of the magnitude of J1820 over the course of a week. In order to perform differential photometry on the source, some non-variable reference stars located in the region of J1820 had to be selected. Because J1820 has a magnitude of 14.2, the reference stars needed to have a similar magnitude as well as a known magnitude in the same filter as the images we have. Selecting the reference stars began by using an astronomical database, SIMBAD, to identify all of the stars in the region and then using another database, Pan-STARRS, to determine the known magnitudes of the stars in the r' filter. Figure 4 is an image in DS9 highlighting the names and locations of the reference stars used in relation to the target source J1820.
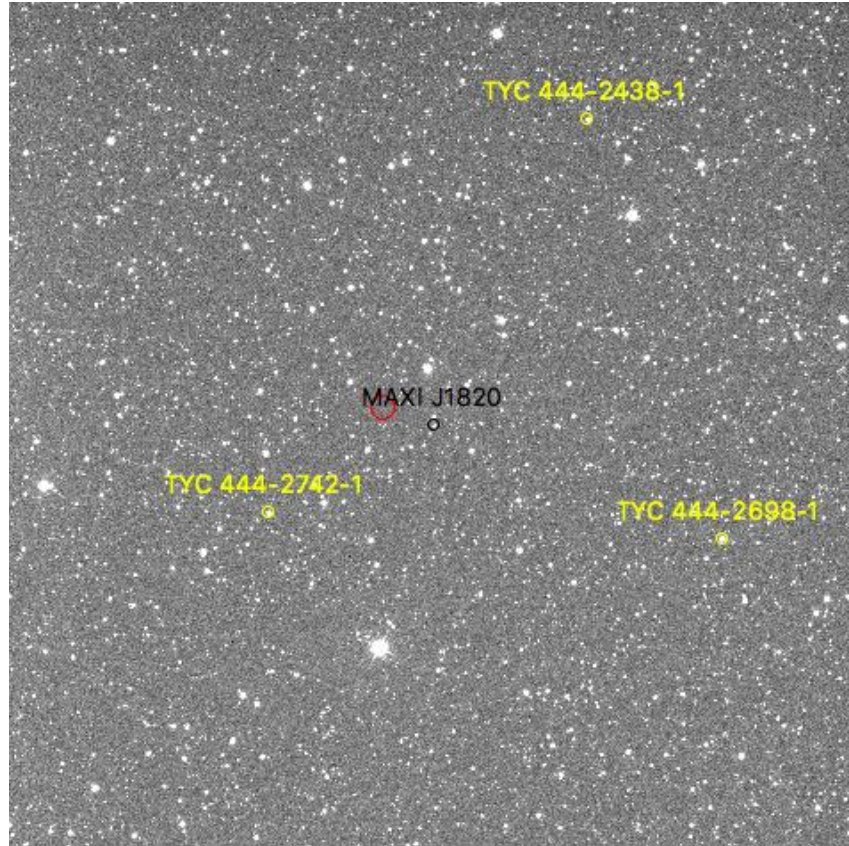
Figure 4: The location of the target source is in black and the location of the reference stars is in yellow. The red region indicates the background location used for the background count subtraction.

A circular region of space with a radius of 12 arcseconds was created around each source and by using an analysis function in DS9, information regarding the number of counts, which is related to the number of photons that hit the detector, and the number of pixels in the region was recorded in a Microsoft Excel file. Once the counts and pixels were recorded for each source, the median number of counts for a region of background, or blank space free of other sources of

light, with a radius approximately double the size of the source regions was also recorded. The purpose of the background region is that it allows for the subtraction of any additional number of counts provided by the backgrounds for the source regions. Figure 4 displays the background region used for each source. The subtraction of background counts was done by taking the product of the area of the sources with the median number of counts for the background and subtracting that value from the total number of counts for each source. Table 1 is an example of the values gathered from one night of observations.

After the background subtraction was calculated for each source, the magnitude of the target star J1820 was calculated with respect to each reference star. The general equation to find the apparent magnitude of a star is given by equation 2:

$$m^* = -2.5 \log_{10}\left(\frac{N_*}{N_i}\right) + m_i \tag{2}$$

Where N_* is the number of counts once the background has been subtracted for the target star and N_i is the number of counts background subtracted for each reference star. m^* and m_i refer to the apparent magnitude of the target star and reference star respectively.


5 Results

Equation 2 was used to find the apparent magnitude of J1820 in the r' filter relative to each reference star and from those values, the average of the magnitudes for each night was calculated. An error bar was given to each average magnitude calculated by the individual standard deviation for each data point. Figure 5 shows the optical light curve of J1820 at the end of the main outburst in October 2018. A least squares fit was added to fit a line to the data points where the value of the slope of the line is 0.0251 days$_{-1}$ and the value of the intercept is -1091.

11
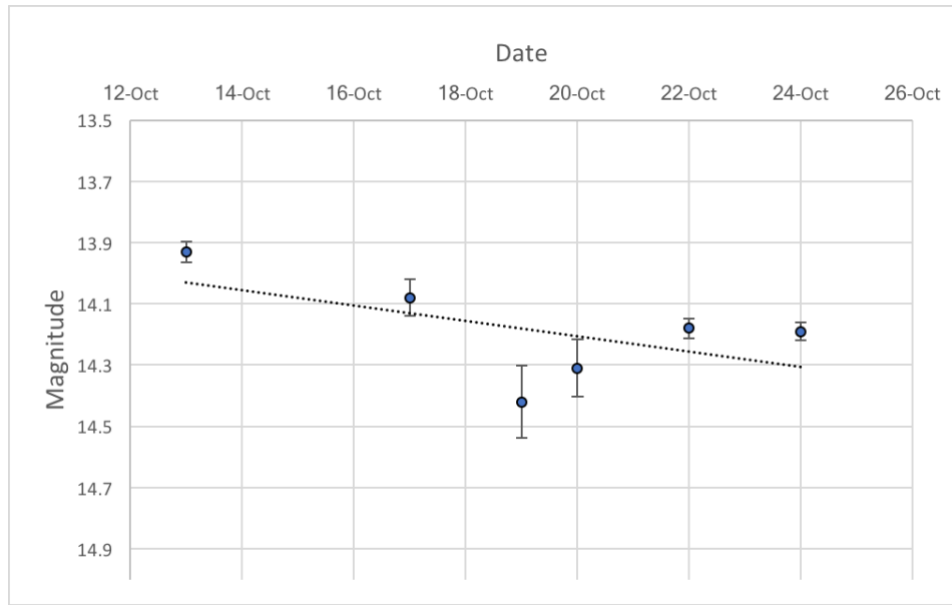
Figure 5: The light curve that was produced indicates that the J1820 system is getting fainter over time. The points are plotted on a logarithmic-linear scale (logarithmic y-axis, linear x-axis) meaning the linear trend of the decay correlates to an exponential decay. Each data point contains an error bar, and it is clear that October 19 and 20 contain large sources of error. This is likely due to the calibrations of the images for those nights.

When analyzing the results of the optical light curve, two dates in particular stand out as deviant. The nights of October 19 and October 20 have large error bars and they are the only two nights that appear to deviate from the linear trend. It is difficult to find a reasonable background region for each of the reference stars and target as the background of the images changes a considerable amount. The most probable reason for such high error on these nights is likely related to the calibration of the images. The images used for both of these nights appear to have a gradient across the image which is likely due inaccurate corrections from the flat fields, however the true reason for the poor image quality is unknown. Figure 6 shows the images used for these nights.
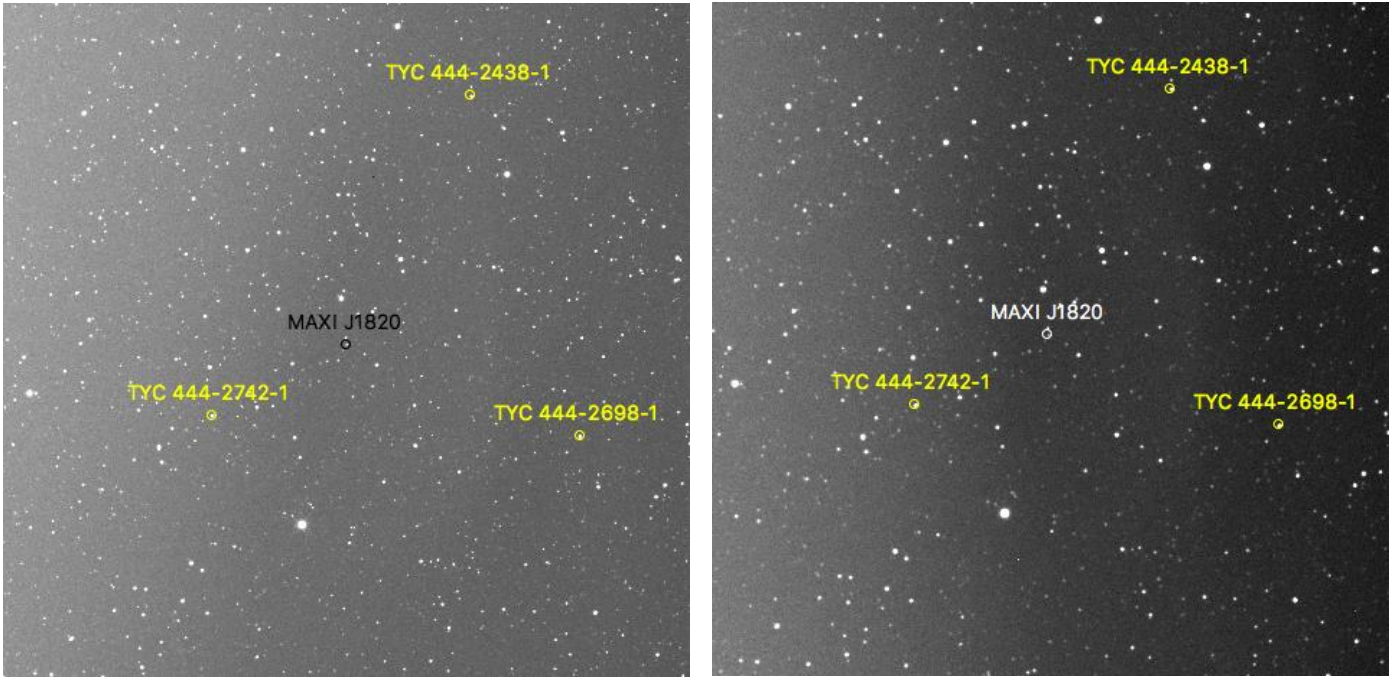
Figure 6: The image on the left shows the image used for calculations on October 19 while the image on the right is the one used for October 20. Although the gradient is more apparent in the right image, both images contain a gradient where the right side is much darker than the left indicating that the images were not properly calibrated. The set of calibrations files received from GBO did not include calibration files from each night of observations so the calibrations for each night may not be reduced accurately.

The graph in Figure 5 is plotted on a logarithmic-linear scale, so the linear trend correlates to an exponential decay. Therefore, from the light curve, it can be concluded that the brightness of J1820 decayed exponentially. The time it takes the brightness to decay was determined by taking the slope of a line of best fit and using equation 3:

$$t_0 = \frac{2.5}{m_o * \ln(10)} \tag{3}$$

Where t_0 is the time it takes the brightness to decay by a factor of e and m_o is the slope of the line from the optical light curve. The resulting timescale for the optical region is a period of around 43 days. Taking the two deviant points into consideration, this result is an underestimate as the deviant points appear to steepen the slope of the light curve which in turn decreases the value of the timescale of decay. These results were then compared to Figure 7, a light curve in the X-ray region produced by Dr. Aarran Shaw, a postdoctoral researcher at UNR. The graph was plotted as total flux versus time rather than magnitude versus time like the optical region.
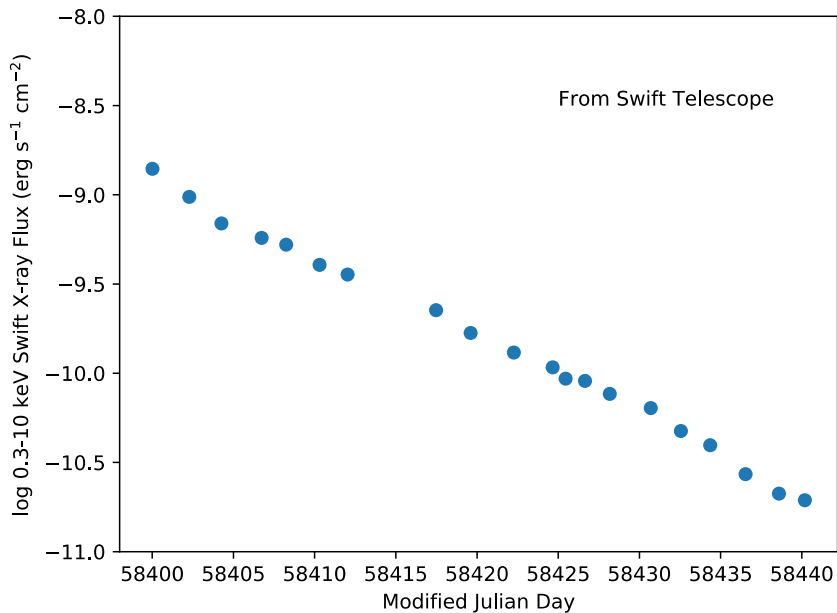
Figure 7: This graph is the light curve of J1820 in the X-ray region plotted as flux versus time. The time it takes the outburst in the X-ray region was calculated similarly to the optical region and was then used for comparison.

The calculated timescale for the X-ray region was found to be about 10 days, which is approximately one-fourth the time it takes the optical region to decay. Potential explanations for these results will be discussed in the following section.

6 Discussion/Conclusions

After analyzing the results of the light curve for the optical region of the outburst for J1820, it has been determined based on the data that the brightness of the optical light decays exponentially with a timescale of approximately 43 days. The time it takes the brightness of the X-ray light to decay is much shorter at around 10 days. There are various potential explanations for these results due to the complexity of the structure of the black hole. The discussions begin with the origin of the optical emission from this system.

One explanation is that the optical light is being emitted from the outer part of the accretion disk through blackbody radiation. The temperature of the accretion disk decreases as the distance from the center of the disk increases, so the wavelengths of light emitted farther away from the center of the disk will be longer than those emitted closer to the center. This would explain that the optical light is being directly emitted from the accretion disk.

Another potential explanation to discuss is the reflection of X-rays off the outer part of the disk. The emission of high energy X-rays comes from the hot corona near the center of the accretion disk which emits the X-rays in all directions. Some of the X-rays can be emitted toward the accretion disk where they will be reflected off the outer part of the disk ultimately releasing optical emission. If this were the case, however, we would see similarities in the timescales of the optical and X-ray decay during the outburst, but given the results of the light curve obtained by the optical light, this may not be the case for J1820.

The final potential explanation for the origin of optical emission comes from the starlight of the companion star. Because the companion star accretes matter onto the black hole, some light from the star can also be emitted and observed. After analyzing data collected once J1820

15

became fainter, it has been determined that the magnitude of J1820 in the r' filter is approximately 17.5 [9] which in turn means the magnitude of the companion star must be greater than this. The light observed during the outburst cannot come from the companion star as the magnitude observed during outburst is much brighter than the magnitude of the companion star.

After considering all of the possibilities of optical emission, the most likely explanation is that the light originates from the blackbody radiation of the accretion disk. The timescales of the optical and X-ray decay were determined to have distinct quantities suggesting that the two regions are independent of one another.

7 References

[1] Atri, P., Miller-Jones, J. C. A., Bahramian, A., Plotkin, R. M., Deller, A. T., Jonker, P. G., … Tudose, V. (2020). A radio parallax to the black hole X-ray binary MAXI J1820 070. *Monthly Notices of the Royal Astronomical Society: Letters*, *493*(1). doi: 10.1093/mnrasl/slaa010

[2] Bessell, M. S. (2005). Standard Photometric Systems. *Annual Review of Astronomy and Astrophysics*, *43*(1), 293–336. doi: 10.1146/annurev.astro.41.082801.100251

[3] Fender, R. (2009). 'Disc–Jet' Coupling in Black Hole X-Ray Binaries and Active Galactic Nuclei. *The Jet Paradigm Lecture Notes in Physics*, 115–142. doi: 10.1007/978-3-540-76937-8_5

[4] Kohler, S. (2018, November 14). A Black Hole X-Ray Binary Rises. Retrieved from https://aasnova.org/2018/11/14/a-black-hole-x-ray-binary-rises/

[5] Malatesta, K. (2010, April 13). W Ursae Majoris. Retrieved from https://www.aavso.org/vsots_wuma

[6] Maoz, D. (2016). *Astrophysics in a Nutshell*. Princeton: Princeton University Press.

[7] Musegades, L., Niebuhr, C., Graham, M., Poore, A., Freed, R., Kenney, J., & Genet, R. (2018, April 1). An Astrometric Observation of Binary Star System WDS 15559-0210 at the Great Basin Observatory. Retrieved from https://ui.adsabs.harvard.edu/abs/2018JDSO...14..197M/abstract

[8] Sun, M., Xue, Y., Brandt, W. N., Gu, W.-M., Trump, J. R., Cai, Z., … Wang, J. (2020). Corona-heated Accretion-disk Reprocessing: A Physical Model to Decipher the Melody of AGN UV/Optical Twinkling. *The Astrophysical Journal*, *891*(2), 178. doi: 10.3847/1538-4357/ab789e

[9] Torres, M. A. P., Casares, J., Jiménez-Ibarra, F., Muñoz-Darias, T., Padilla, M. A., Jonker, P. G.,

    & Heida, M. (2019). Dynamical Confirmation of a Black Hole in MAXI J1820 070. *The*

    Astrophysical Journal, *882*(2). doi: 10.3847/2041-8213/ab39df

[10] Tucker, M. A., Shappee, B. J., Holoien, T. W.-S., Auchettl, K., Strader, J., Stanek, K. Z., …

    Dage, K. (2018). ASASSN-18ey: The Rise of a New Black Hole X-Ray Binary. *The*

    Astrophysical Journal, *867*(1). doi: 10.3847/2041-8213/aae88a